Contract No:

This document was prepared in conjunction with work accomplished under Contract No. DE-AC09-08SR22470 with the U.S. Department of Energy (DOE) Office of Environmental Management (EM).

Disclaimer:

We put science to work.™

Savannah River National Laboratory™

OPERATED BY SAVANNAH RIVER NUCLEAR SOLUTIONS

A U.S. DEPARTMENT OF ENERGY NATIONAL LABORATORY • SAVANNAH RIVER SITE • AIKEN, SC

Thermal Performance Analysis of a Geologic Borhole Repository

Lauren Reagin*

* Summer Intern Student

Mentor: Si Young Lee

August 2016

SRNL-STI-2016-00457, Revision 0

DISCLAIMER

Printed in the United States of America

Prepared for
U.S. Department of Energy

SRNL-STI-2016-00457
Revision 0

Keywords: *Thermal Analysis, Borehole, Waste Package, DSRS*

Retention: *Permanent*

Thermal Performance Analysis of a Geologic Borehole Repository

Lauren Reagin*

* Summer Intern Student

Mentor: Si Young Lee

August 2016

Prepared for the U.S. Department of Energy under contract number DE-AC09-08SR22470.

REVIEWS AND APPROVALS

AUTHORS:

_____

L. Reagin, Environmental Modeling Date

TECHNICAL REVIEW:

_____

S. Y. Lee, Environmental Modeling Date

APPROVAL:

_____

D. A. Crowley, Manager Date
Environmental Modeling

EXECUTIVE SUMMARY

The Brazilian Nuclear Research Institute (IPEN) proposed a design for the disposal of Disused Sealed Radioactive Sources (DSRS) based on the IAEA Borehole Disposal of Sealed Radioactive Sources (BOSS) design that would allow the entirety of Brazil's inventory of DSRS to be disposed in a single borehole. The proposed IPEN design allows for 170 waste packages (WPs) containing DSRS (such as Co-60 and Cs-137) to be stacked on top of each other inside the borehole.

The primary objective of this work was to evaluate the thermal performance of a conservative approach to the IPEN proposal with the equivalent of two WPs and two different inside configurations using Co-60 as the radioactive heat source. The current WP configuration (heterogeneous) for the IPEN proposal has 60% of the WP volume being occupied by a nuclear radioactive heat source and the remaining 40% as vacant space. The second configuration (homogeneous) considered for this project was a homogeneous case where 100% of the WP volume was occupied by a nuclear radioactive heat source. The computational models for the thermal analyses of the WP configurations with the Co-60 heat source considered three different cooling mechanisms (conduction, radiation, and convection) and the effect of mesh size on the results from the thermal analysis.

The results of the analyses yielded maximum temperatures inside the WPs for both of the WP configurations and various mesh sizes. The heterogeneous WP considered the cooling mechanisms of conduction, convection, and radiation. The temperature results from the heterogeneous WP analysis suggest that the model is cooled predominantly by conduction with effect of radiation and natural convection on cooling being negligible. From the thermal analysis comparing the two WP configurations, the results suggest that either WP configuration could be used for the design. The mesh sensitivity results verify the meshes used and results obtained from the thermal analyses were close to being independent of mesh size. The results from the computational case and analytically-calculated case for the homogeneous WP in benchmarking were almost identical, which indicates that the computational approach used here was successfully verified by the analytical solution.

TABLE OF CONTENTS

LIST OF FIGURES

LIST OF TABLES

LIST OF ABBREVIATIONS AND NOMENCLATURE

CFD	Computational Fluid Dynamics
WP	Waster Package
Co-60	Cobalt 60
Cs-137	Cesium 137
IAEA	International Atomic Energy Agency
BOSS	Borehole Disposal of Disused Sealed Sources
DSRS	Disused sealed radioactive sources
IPEN	Instituto de Pesquisas Energeticas e Nucleares
k	Thermal conductivity
q_{cond}	Conductive heat flux
q_{rad}	Radiative heat flux
Q_{load}	Total heat loading (watts)
q'''	Heat source per unit volume
r	Radial direction along the radial coordinate
T_{wall}	Temperature of the wall of the WP
∇	Gradient operator
ρ	Density
ν	Kinematic viscosity
Ra	Rayleigh number
Gr	Grashoff number
Pr	Prandtl number
g	Gravity
T_{wall}	Temperature of the wall of the WP
T_{avg}	Average temperature over the WP region
x	Length of the entire WP
α	Thermal diffusivity
β	Thermal expansion coefficient

1.0 Introduction

This document describes the computational models for the thermal analyses of Waste Packages (WPs) carrying Co-60 in a simplified model of a geological repository. The original concept of this model was based on a modification of the the International Atomic Energy Agency (IAEA) Borehole Disposal of Sealed Radioactive Sources (BOSS) design that allows for the safe and permanent disposal of Disused Sealed Radioactive Sources (DSRS) in a borehole [1]. The modifications from the BOSS model that was proposed by the Instituto de Pesquisas Energeticas e Nucleares (IPEN) will allow the disposal of the DSRS, which includes Co-60 and Cs-137, found in Brazil in a single borehole that will contain 170 WPs [2].

The modified BOSS model was then simplified even more to allow for a more conservative approach. The simplified model includes only two WP's that contain Co-60 due to its high heat generation. Therefore, the temperature distribution and the effects of conduction, convection, and radiation are important aspects of interest for this project. All computational analyses and modeling geometry creations are performed by a commercial Computational Fluid Dynamics (CFD) software, ANSYS-FLUENT [4].

2.0 Modeling Geometry and Solution Approach

The original concept based on the IPEN proposal of the BOSS modification involved a configuration of 170 WPs in a single vertical borehole. Each WP (Figure 1) has a cylindrical geometry with a volumetric capacity of 1.54 liters, corresponding to its 51 mm radius and 189 mm height. About 60% of each WP is occupied by a nuclear radioactive heat source with the remaining 40% of the WP volume is vacant space [2].

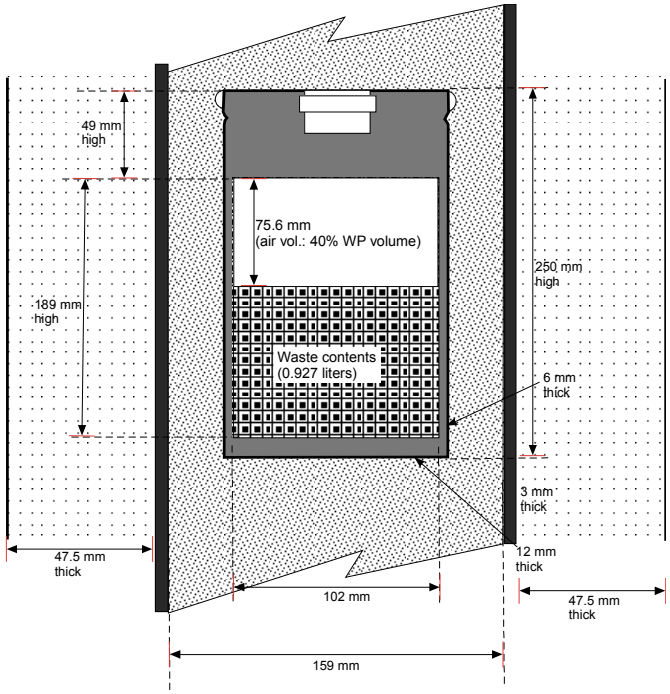

Figure 1: WP Components of IPEN Proposal [2].

A Computational Fluid Dynamics (CFD) method using ANSYS Fluent, which is a full Navier-Stokes based equation solver, with axisymmetric steady-state method approach was used for computational efficiency for the thermal modeling calculations [4]. The calculations in ANSYS Fluent were performed under the conduction-convection-radiation model for the heterogeneous WP. The calculations in ANSYS fluent were performed under the conduction model for the homogeneous WP.

The steady-state equation governing the conduction-convection-radiation heat transfer problem of the WP under the axisymmetric cylindrical coordinate system can be seen in Equation 1.

$$\rho C_p \left(v_r \frac{\partial T}{\partial r} + v_z \frac{\partial T}{\partial z} \right) + \nabla * (\bar{q}_{cond} + \bar{q}_{rad}) - q''' = 0 \quad (1)$$

In Equation (1), v_r and v_z represent convective velocities along the radial and axial directions, respectively. $\bar{q}_{cond}$ is the conductive heat flux term calculated by the product of spatial temperature gradient and thermal conductivity k. The radiation heat flux term $\bar{q}_{rad}$ was calculated by the Discrete Ordinate (DO) method [4]. Decay heat source term q''' is provided to the energy equation as a model input.

The setup of the modeling calculation requires the input of thermal and material properties of the WP and its components, boundary conditions, and thermal loading within the established modeling domain. These input parameters will be discussed further into the paper.

2.1 Modeling Geometry

The entire modeling domain consisted of the WP container (top, bottom, side casing, waste region, and vacant region if applicable), the casing backfill, the borehole casing, the casing grout, the borehole, and 50 meters of granite. The WP components can be seen in Figure 1 with the dimensions and materials listed below [1, 2].

Waste Package (container)

- OD – 114 mm
- ID – 102 mm
- Height – 250 mm
- Wall Thickness – 6 mm
- Top Thickness – 49 mm
- Bottom Thickness – 12 mm
- Stainless Steel

Casing Backfill

- Around Thickness – 22.5 mm
- Cement Grout

Borehole Casing

- OD – 165 mm
- ID – 159 mm
- Wall Thickness – 3 mm
- Stainless Steel

Casing Grout
- Diameter – 47.5 mm
- Height – 250 mm
- Cement Grout

Borehole
- Internal Diameter – 260 mm

Granite
- Height – 50 m
- Granite

The geometry was created and meshed using the ANSYS Gambit software. The geometry was simplified from the original concept to the equivalent of 2 WPs containing Co-60 in order to apply a conservative approach. A homogeneous case (100% WP) was done in order to compare with the non-homogeneous case (60% WP, 40% air).

There are portions of the modeling domain that are decomposed into component surfaces to allow greater mesh accuracy and efficiency. In the regions that are expected to experience larger temperature gradients and/or velocity due to natural convection, the component is assigned a greater mesh density to increase the accuracy of the solution. The vacant air region in the heterogeneous WP has a greater mesh density with a bias towards top and bottom of the vacant air region and towards the WP wall due to interest in both temperature and velocity. An edge sizing method is used for the majority of the components, but a pave method is used for the casing backfill grout and the granite region. A coarse mesh and fine mesh were used with each WP configuration to prove the validity of the findings do not vastly vary with the amount of control volumes. The heterogeneous WP has a coarse mesh with 43, 605 elements and a fine mesh with 344,438 elements. The homogeneous WP has a coarse mesh with 60,070 elements and a fine mesh with 206,187 elements. The coarse and fine mesh for the heterogeneous WP can be seen in Figure 2. The coarse and fine mesh for the homogeneous WP can be seen in Figure 3.

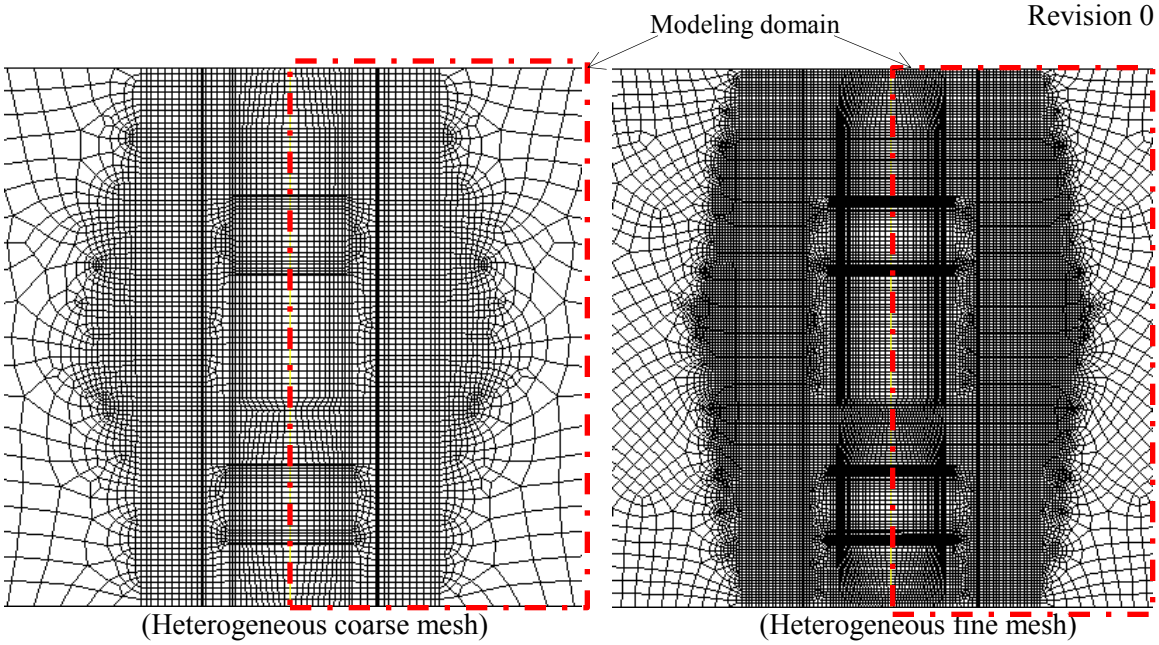

Figure 2. The computational meshes over the modeling domain of the heterogeneous WP including the WP, borehole, and a portion of the granite (Yellow line: axisymmetric line).

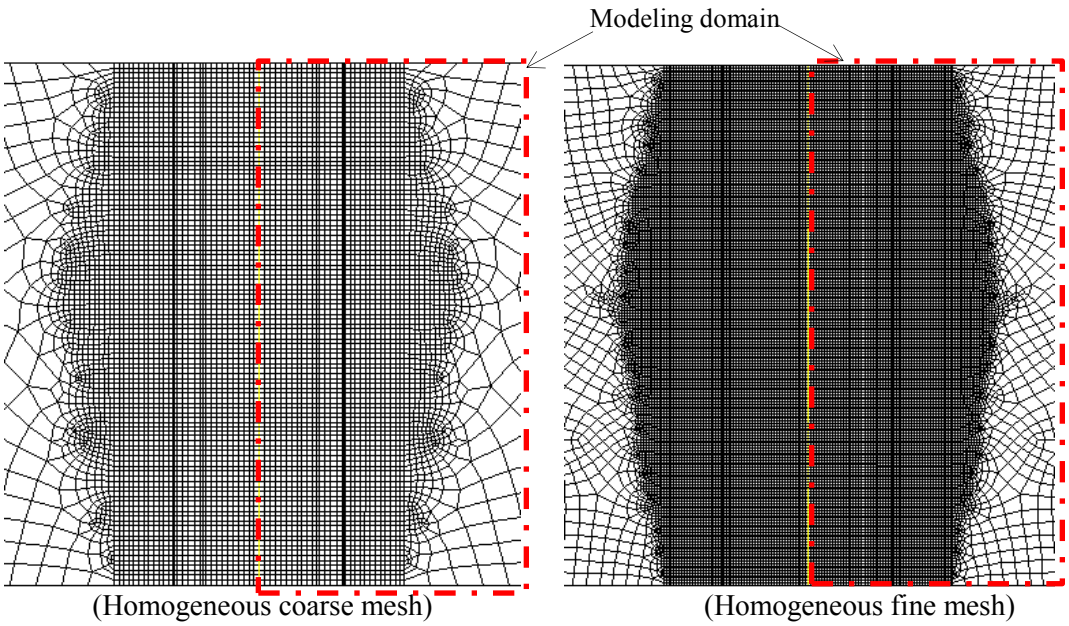

Figure 3. The computational meshes over the modeling domain of the homogeneous WP including the WP, borehole, and a portion of the granite (Yellow line: axisymmetric line).

2.2 Boundary Conditions

For a conservative approach, the top boundary wall and bottom boundary wall of the WP domain were set to being adiabatic (q’’’=0). For the calculations, the WPs were in an upright position and were stored in the borehole with 50 meters of granite on the outside of the borehole. The granite boundary wall had an initial temperature of 308.95 K, which was obtained from given geological data from Brazil. Due to the borehole and WP container being cylindrical, the energy transfer within the WP was symmetric about the central axis of the WP. This allowed for an axisymmetric

analysis of one-half of the WP, which decreased the time needed for calculations. The cooling mechanisms within the WP were conduction/radiation and natural convection due to gravity.

2.3 Material Properties

Material and thermal properties used for the thermal analyses of the heterogeneous WP are in Table 1 and the heat source terms associated with different regions of the WP are listed in Table 2[2]. There was radioactive material of Co-60 in the WP that is a primary heat source of radioactive decay. There were secondary heat sources due to gamma interaction in the WP side casing, the casing backfill grout, and the casing grout. The vacant space in the heterogeneous WP was filled with air for a conservative approach. The vacant space was filled with helium as a sensitivity case due to helium being inert with a higher thermal conductivity (k_{helium} = 0.152 W/m-K), which lowers maximum temperatures[3]. The emissivity for the WP wall of the vacant region was 0.3[2]. For the homogeneous WP, the thermal conductivity for the stainless steel WP walls and the volumetric heat flux of the Co-60 source decreased due to the combination of the vacant region and waste package region. Material and thermal properties used for the thermal analyses of the homogeneous WP are in Table 3 and the heat source terms associated with different regions of the WP are listed in Table 4[2].

Table 1: Material and thermal properties used for the analysis of the heterogeneous WP case [2].

Material	Thermal Conductivity (W/m-K)	Density (kg / m^3)	Specific Heat (J/kg-K)
Concrete	1.5	2400	750
Stainless Steel	16.3	7913	565
Granite	3.2	2600	837
Air	0.03	Ideal gas	1000

Table 2: Heat source terms for the heterogeneous WP containing Co-60 [2].

Co-60 TBq: 9.66E+01, # of WP's: 2 WP's				
Location	*Source***	*WP*	*Inner Grout*	*Outer Grout*
Density* [g/cc]	8.00	8.00	3.29	3.29
mass [kg]	7.45	6.94	8.106	27.3
F6 Rad/hr	1.03E+06	2.31E+05	1.57E+05	4.67E+04
rad/s	2.86E+02	6.41E+01	4.37E+01	1.30E+01
J/kg/s	2.86E+00	6.41E-01	4.37E+00	1.30E-01
W per package	22.80	4.45	4.45	3.54
W/Liter	**24.49**	**5.13**	**1.44**	**0.43**
% deposit in location	59.01%	11.51%	9.17%	9.17%

Note: *Assuming steel density for conservative gamma deposition
** Source heat includes average Beta energy as well (1.48 for Co-60)

Table 3: Material and thermal properties used for the analysis of the homogeneous WP case [2].

Material	Thermal Conductivity (W/m-K)	Density (kg/m^3)	Specific Heat (J/kg-K)
Concrete	1.5	2400	750
Stainless Steel	16.3	7913	565
Stainless Steel Homogeneous	9.792*	7913	565
Granite	3.2	2600	837

Note: * Thermal conductivity decreased for the stainless steel used for the homogeneous waste package due to the combination of the air region and waste package region.

Table 4: Heat source terms for the homogeneous WP containing Co-60 [2].

Co60 TBq: 9.66E+01, # of WP's: 2 WP's				
Location	*Source***	*WP*	*Inner Grout*	*Outer Grout*
Density* [g/cc]	8.00	8.00	3.29	3.29
mass [kg]	7.45	6.94	8.106	27.3
F6 Rad/hr	1.03E+06	2.31E+05	1.57E+05	4.67E+04
rad/s	2.86E+02	6.41E+01	4.37E+01	1.30E+01
J/kg/s	2.86E+00	6.41E-01	4.37E+00	1.30E-01
W per package	22.80	4.45	4.45	3.54
W/Liter	**14.694**	**5.13**	**1.44**	**0.43**
% deposit in location	59.01%	11.51%	9.17%	9.17%

Note: *Assuming steel density for conservative gamma deposition
** Source heat includes average Beta energy as well (1.48 for Co-60)

3.0 Results and Discussions

The following sections describe the resulting data of the thermal analyses done for the Co-60 WPs. Section 3.1 describes a benchmarking case of a single homogeneous WP with analytical calculations compared to computational calculations using ANSYS Fluent. Section 3.2.1 describes the thermal performance analysis of the heterogeneous WP with the analysis of the different cooling mechanisms (conduction, radiation, convection) and the effects of mesh size. Section 3.2.2 describes the thermal performance analysis for a homogeneous WP case where the airspace was removed in order to compare to the thermal analysis of the heterogeneous WP case. Section 3.2.3 describes a mesh sensitivity analysis for the vacant space filled with air in the heterogeneous WP. Section 3.2.4 describes a mesh sensitivity analysis for the Co-60 source region in the homogeneous WP.

3.1 Benchmarking

A benchmarking case was completed to test the validity of the computed values obtained from the CFD simulations versus a hand-calculated analytical solution. A simplified model of a single homogeneous WP configuration was modeled and compared to values obtained from the same single homogeneous WP configuration solved by hand. The configuration of the WP only

included the source region (R = .051 m) and the WP wall (d = .006 m). The assumptions for the calculations were: steady-state, conduction only, constant thermal conductivity, and symmetric about r = 0. The geometry and setup values of the single homogeneous WP can be seen in Figure 4.

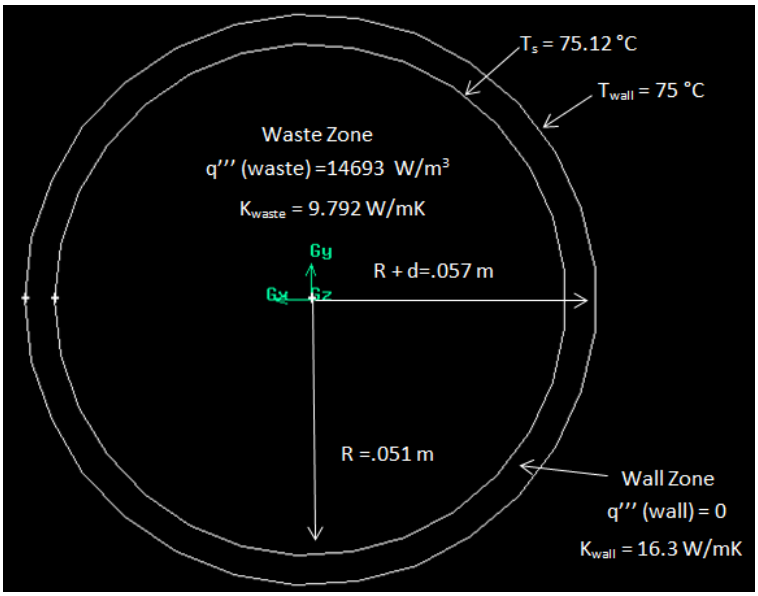

Figure 4. The geometry of the homogeneous WP and the setup values for benchmarking.

For the hand-solved calculations, the heat conduction equation (see Equation 2) with cylindrical coordinates was solved using the following boundary conditions:

$$BC\ 1: T(r = R) = T_s$$

$$BC\ 2: \frac{\partial T}{\partial r}\ (@\, r = 0) = 0$$

$$BC\ 3: T(r = R + d) = T_{wall}$$

$$BC\ 4: q''_{wall}(@\, r = R + d) = -k_{wall}\frac{dT}{dr}$$

$$\frac{1}{r}\frac{\partial}{\partial r}\left(r\frac{\partial r}{\partial t}\right) + \frac{q'''}{k} = 0 \qquad (2)$$

The hand-solved equation was a piece-wise function that was split up into the waste region and the wall region. The waste region portion of the piecewise equation depended on the temperature of the surface region of the waste, the volumetric heat flux (q’’’) of the waste, the thermal conductivity of the waste, the radius (R) of the wall region, and the position of the variable radius (r). The wall region portion of the piecewise equation depended on the temperature of the wall, the volumetric heat flux (q’’’) of the waste, the thermal conductivity of the wall, the radius of the wall region (R+d), and the position of the variable radius (r). The piecewise equation can be seen in Equation 3.

$$T(r) = \begin{cases} T_s + \frac{q'''}{4k_{waste}}(R^2 - r^2), & 0 \le r < R \\ T_{wall} + \frac{q'''R^2}{2k_{wall}} \ln\left(\frac{R+d}{r}\right), & R \le r \le R+d \end{cases} \quad (3)$$

The computational model was set up to correspond with the setup of the hand-solved calculations. The geometry was completed in Gambit software [4] while the simulation was completed using ANSYS Fluent. The waste region mesh used a pave method with interval sizes of 2.67 mm. The wall region was decomposed into component surfaces to allow for easier meshing and a paved method was used for the mesh with interval sizes of 2.67 mm. For the simulation, the material properties for the homogeneous WP case (Tables 3 & 4) were used, the model was ran with conduction only, and the only heat source for the model was from the Co-60 in the waste region. The mesh for the single homogeneous WP can be seen in Figure 5.

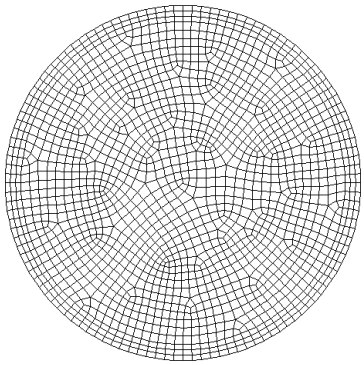

Figure 5. The computational mesh generated for the single homogeneous WP.

To compare the analytical solution and the CFD model case, two non-dimensional parameters were used to quantify them on the same scale. The first non-dimensional parameter was dependent on the temperature, while the second non-dimensional parameter was dependent on the radius. With the two cases quantified on the same scale, the radius non-dimensional parameter was plotted against the temperature non-dimensional parameter to observe how the temperature changes from the middle of the waste region to the edge of the wall. The results from the two cases were almost identical, which indicates that the computational approach used was successfully comparable to the hand-calculated approach. The non-dimensional parameter for the temperature can be seen in Equation 4. The non-dimensional parameter for the radius can be seen in Equation 5. The setup values used for the non-dimensional paramaters can be seen in Table 5. The graph of the radius non-dimensional parameter versus the temperature non-dimensional parameter can be seen in Figure 6.

$$\theta = \frac{T(r) - T_{wall}}{T_{max} - T_{wall}} \quad (4)$$

$$\eta = \frac{r}{R+d} \quad (5)$$

Table 5. The values used for the calculation of the non-dimensional parameters of the single homogeneous WP.

	Twall (°C)	Tmax (°C)	T(r) (°C)	R+d (m)	r (m)
Computational	75	76.08	Position dependent	0.057	Position dependent
Hand-solved	75	76.10	Position dependent	0.057	Position dependent

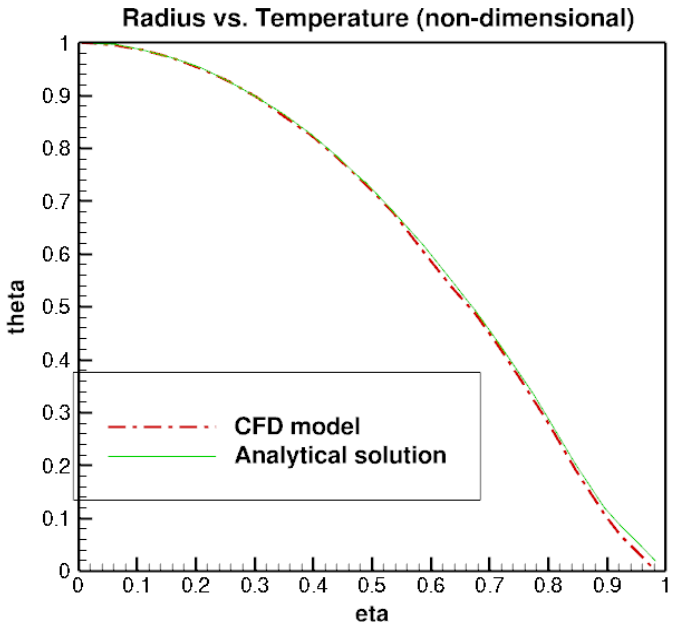

Figure 6. The radius non-dimensional parameter versus the temperature non-dimensional parameter for the single homogeneous WP.

3.2 Thermal Performance Analysis

Since the analytical approach verified the results from the CFD model, the models were validated for use in the thermal performance analysis. The first thermal performance analysis was for the heterogeneous WP, which is the current WP configuration proposed by IPEN. The second thermal performance analysis was a comparison of the heterogeneous WP configuration to a homogeneous WP configuration. The last portions of the thermal performance analysis was a mesh sensitivity analysis for both WP configurations to verify the mesh sizes and the results obtained with the meshes.

3.2.1 Heterogeneous WP Thermal Performance Analysis

A thermal performance analysis was done for the heterogeneous case where the effects of different heat transfer cooling mechanisms were tested as well as the effects of the mesh size. The initial case for the heat transfer methods included conduction, convection, and radiation. The other cases included a conduction + convection model, a conduction + radiation model, and a conduction only model. There was a coarse mesh model of 43, 605 elements and a fine mesh model of 344,438 elements. The initial case with all heat transfer methods experienced the lowest

maximum temperatures of 89.88 °C for the coarse mesh model and 90.27 °C for the fine mesh model. The conduction only case experienced the highest maximum temperatures of 89.93 °C for the coarse mesh model and 90.33 °C for the fine mesh model. Because of the minimal change in temperature between the cases for both mesh models, the cooling method for the WP is prominently conduction dominant. The effect of radiation as a cooling mechanism was negligible due to the low temperature gradient between the source and the WP wall. Radiation has a greater cooling effect in higher temperature cases with a greater temperature gradient. The effect of natural convection as a cooling mechanism was negligible due to the minimal size of the air space. The smaller air space decreases the buoyancy and temperature distribution, which causes an insignificant amount of convection contribution. The calculated values from the heat transfer cases for the coarse heterogeneous mesh can be found in Table 6. The calculated values from the heat transfer cases for the fine heterogeneous mesh can be found in Table 7. The temperature contour distribution comparison of the coarse heterogeneous mesh and fine heterogeneous mesh can be found in Figure 7.

Table 6. Calculated values for the different heat transfer cases for the coarse heterogeneous mesh.

	Max Temperature (°C)	Max Velocity (m/s)	Total Thermal Loading (W)
All	89.88	0.047393	69.49
Cond + Conv	89.91	0.047741	69.49
Cond + Rad	89.90	0	69.49
Cond	89.93	0	69.49

Table 7. Calculated values for the different heat transfer cases for the fine homogeneous mesh.

	Max Temperature (°C)	Max Velocity (m/s)	Total Thermal Loading (W)
All	90.27	0.0518	69.49
Cond + Conv	90.30	0.0522	69.48
Cond + Rad	90.29	0	69.48
Cond	90.33	0	69.49

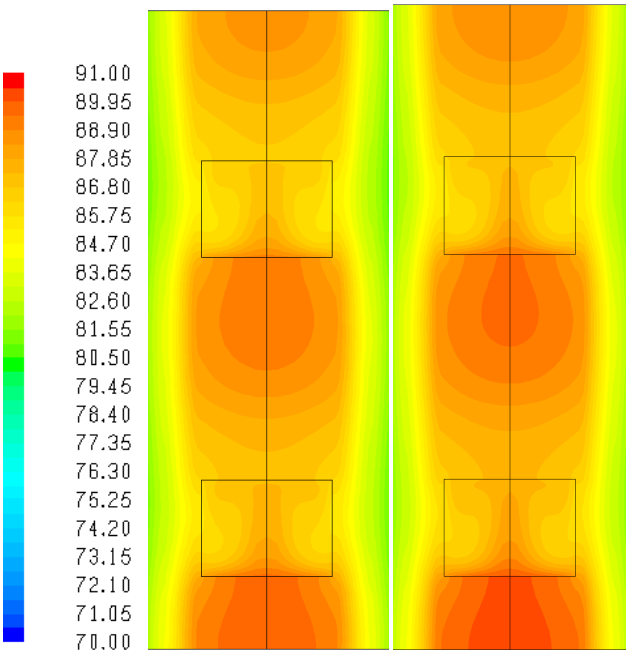

Figure 7. Temperature (°C) contours of the entire WP region for the heterogeneous WP case.

Because air has a lower thermal conductivity (.03), the heat transfer rate through air is very slow. Helium is an ideal choice for the vacant space as it is inert and has a higher thermal conductivity (0.152). Therefore the simulation of the fine heterogeneous WP was simulated again with helium in the vacant space of the WP instead of air with conduction, convection, and radiation included. The maximum temperature of the helium case was 90.25 °C, which was only slightly lower than the maximum temperature of 90.27 °C for the initial case with air in the vacant space. The minimal change in temperature between the helium case and initial air case further supports that the effect of natural convection was an insignificant cooling mechanism.

While the effect of natural convection as a cooling mechanism was proved negligible, the velocity and temperature profiles of the vacant air region were still of interest. The gravitational force combined with the density gradient of the air causes buoyancy forces which induces natural (free) convection currents inside the vacant space. The air patterns within the vacant region can be seen flowing in a vortex pattern, with the highest velocity towards the top portion of the vacant region along the axis of symmetry. The temperature contour of the air region shows a similar vortex pattern when compared to the velocity flow pattern. The airflow velocity magnitude vectors inside the vacant space can be seen in Figure 8. The temperature contour inside the vacant space can be seen in Figure 9.

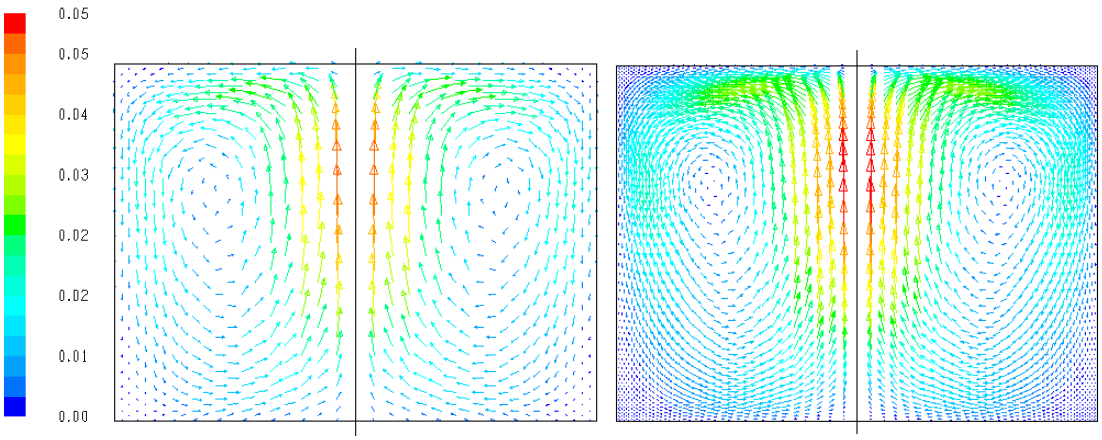

Figure 8. The airlofw velocity (m/s) magnitude vectors inside the vacant space of the heterogeneous WP.

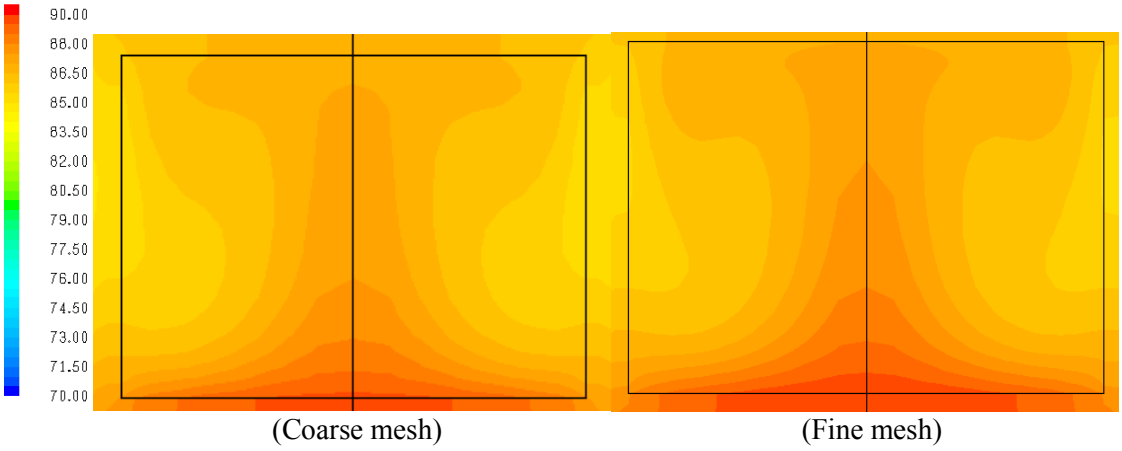

Figure 9. Temperature (°C) contours of the vacant space of the heterogeneous WP.

The Rayleigh (Ra) number is a non-dimensional number of the buoyancy forces over the viscous forces. The number is calculated by multiplying the Grashof (Gr) and Prandtl (Pr) numbers. The Ra number was calculated based on the fine heterogeneous model with air in the vacant space. The Ra number calculated was 26,422.6, which was significantly less than 10^9. This indicates that the flow was laminar and that the buoyancy forces had little effect. The equation for the Rayleigh number can be seen in Equation 6. The values plugged into the Rayleigh number equation can be seen in Table 8.

$$Ra = GrPr = \left(\frac{g\beta}{\nu^2}\right)\left(T_{wall} - T_{avg}\right)\left(x^3\right)\left(\frac{\nu}{\alpha}\right) \quad (6)$$

Table 8. The values plugged into the Rayleigh number equation.

$\frac{g\beta}{\nu^2}$	T_{wall}	T_{avg}	x	$\frac{\nu}{\alpha} = Pr$
5.61 x 10^7	88.5 °C	87 °C	.0756 m	0.7

3.2.2 Heterogeneous WP vs. Homogeneous WP Thermal Performance Analysis

A thermal performance analysis was also done for a homogeneous case where the airspace was removed in order to compare the temperature distribution inside the WP to the temperature distribution of the WP obtained for the heterogeneous case. The simulation included only conduction in the model as the heat transfer method was concluded to be conduction dominant during the heterogeneous WP thermal analysis. The homogeneous WP had a coarse mesh with 60,070 elements and a fine mesh with 206,187 elements. The maximum temperature of the coarse mesh homogeneous WP was 88.37 °C, which was 1.509 °C lower than the maximum temperature of the coarse mesh heterogeneous WP (89.88 °C). The maximum temperature of the fine mesh homogeneous WP was 88.71 °C, which was 1.555 °C lower than the maximum temperature of the fine mesh homogeneous WP (90.27 °C). Because the maximum temperature difference was minimal between the two WP configurations, there is indication that either WP configuration could be chosen. The temperature contour distribution comparison of the coarse mesh heterogeneous WP and coarse mesh homogeneous WP can be found in Figure 10. The temperature contour distribution comparison of the fine mesh heterogeneous WP and fine mesh homogeneous WP can be found in Figure 11.

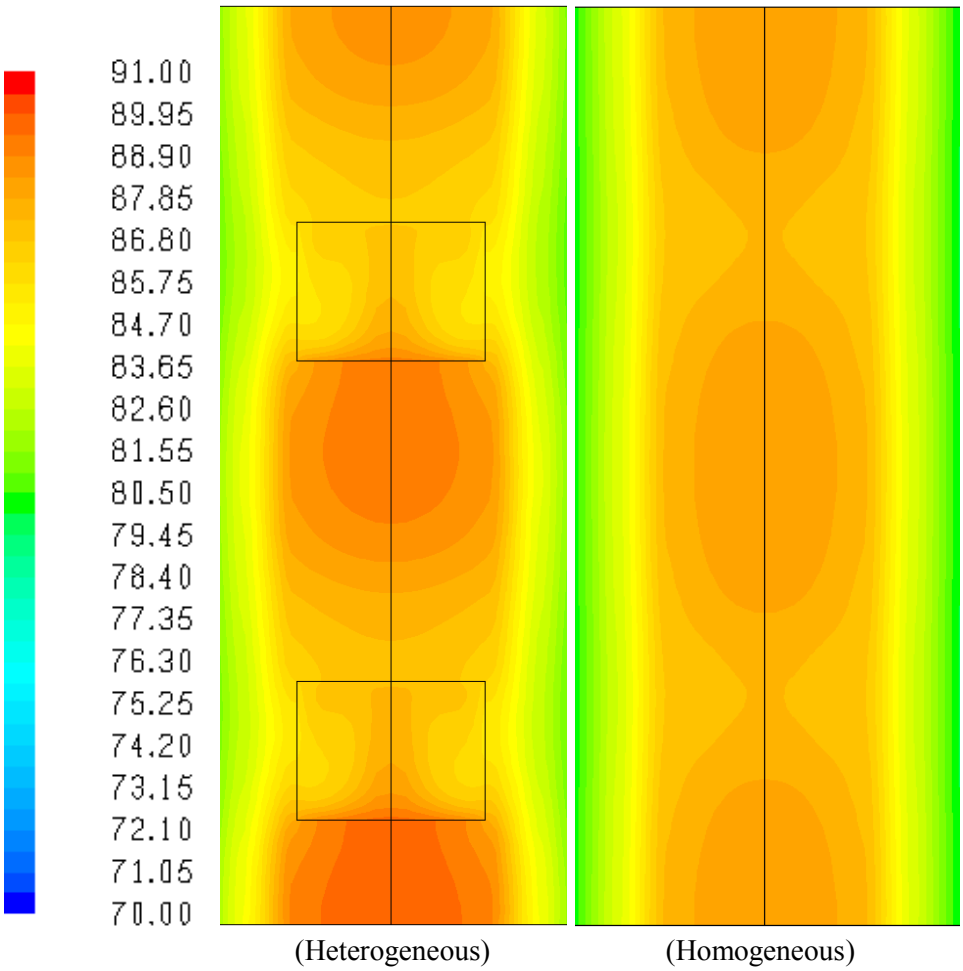

Figure 10.Temperature (°C) contours of the entire WP region for the coarse mesh heterogeneous WP case and coarse mesh homogeneous WP case.

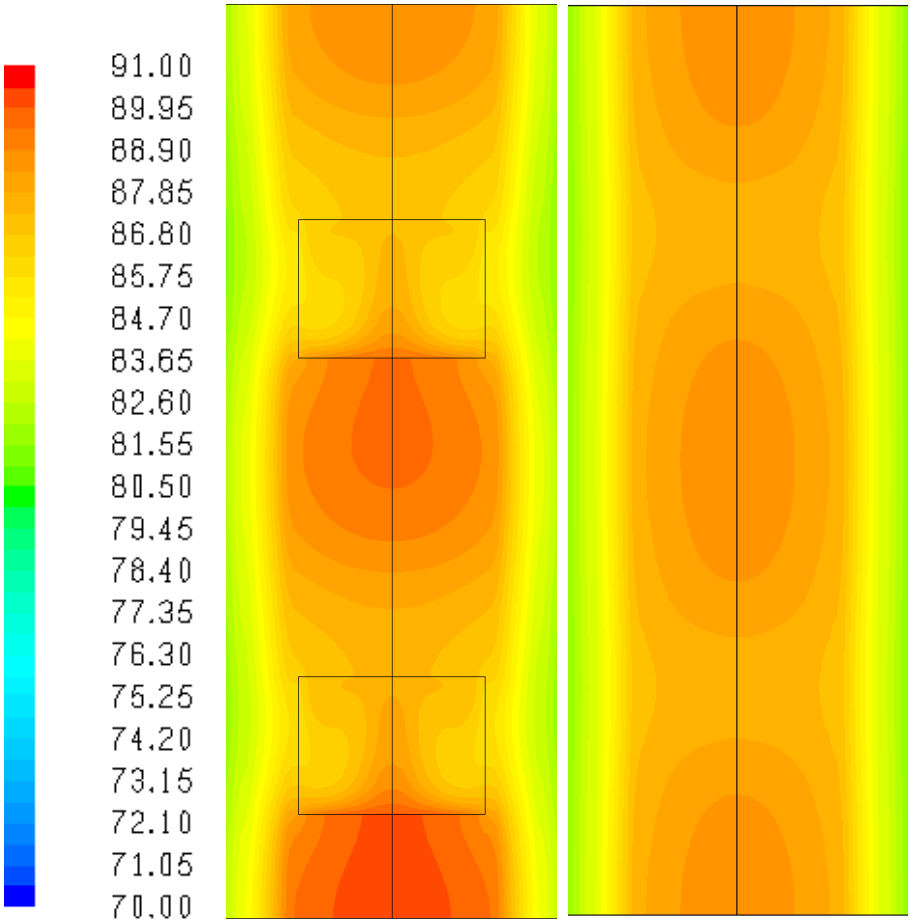

Figure 11. Temperature (°C) contours of the entire WP region for the fine mesh heterogeneous WP case and fine mesh homogeneous WP case.

The temperature distribution from the center of the WP to the casing grout was important due to the cement material used for the casing grout starts to corrode and breakdown at around 65 °C. The decomposition of the casing grout lessens the strength of the total borehole assembly and increases the permeability of the surrounding area. Graphs were made containing the temperature distribution from the central symmetry axis of the middle WP that goes through the WP, casing backfill, borehole casing, and casing grout. For the fine mesh heterogeneous WP, the temperature range of the casing grout was 82.77 °C to 76.56 °C. For the fine mesh homogeneous WP, the temperature range of the casing grout was 82 °C to 76.38 °C. Both of these cases had temperature ranged that were too high for the casing grout region, however this high temperature range was attributed to the approach of the model being too conservative. The graph containing the temperature distribution from the central symmetry axis of the middle WP to the casing grout for the fine mesh heterogeneous WP can be seen in Figure 12. The graph containing the temperature distribution from the central symmetry axis of the middle WP to the casing grout for the fine mesh homogeneous WP can be seen in Figure 13.

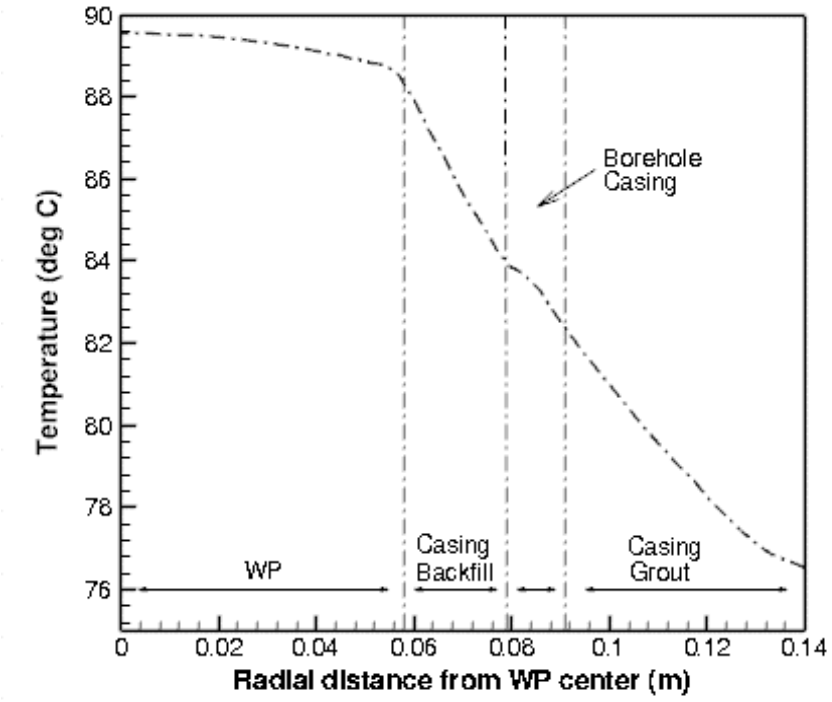

Figure 12. Radial distance from WP center (m) vs. Temperature (°C) of the fine mesh heterogeneous WP.

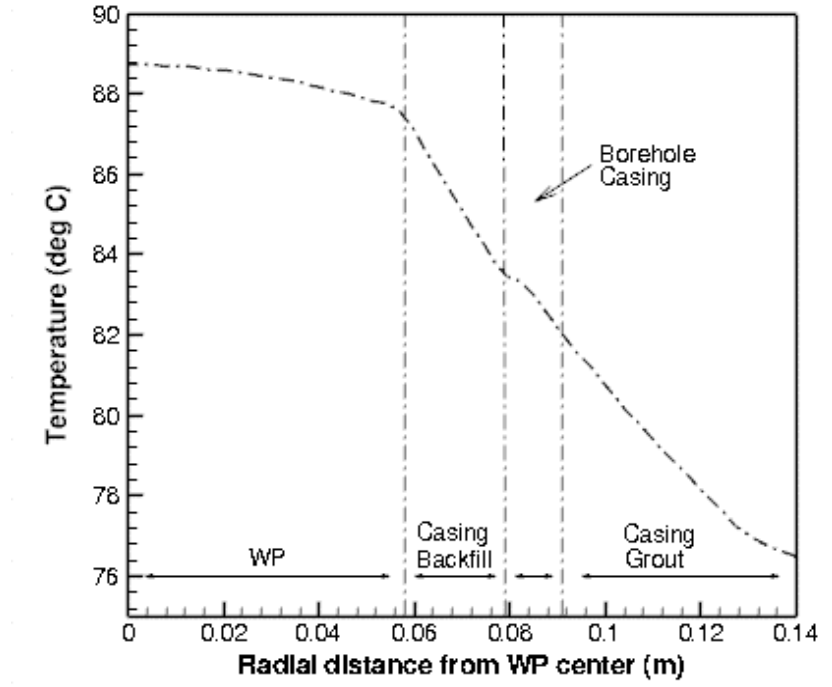

Figure 13. Radial distance from WP center (m) vs. Temperature (°C) of the fine mesh homogeneous WP.

3.2.3 Heterogeneous WP Mesh Sensitivity Analysis

A mesh sensitivity analysis was done for the vacant space filled with air of the heterogeneous WP case in order to verify the validity of the results that were obtained were close to being independent of mesh size. Three different mesh sizes were tested for the vacant space with a bias towards top and the bottom. The mesh sizes of the vacant space were 200 mesh elements, 500 mesh elements, and 800 mesh elements. The maximum temperature changed 0.31 °C between 200 mesh elements and 800 mesh elements. The maximum velocity changed .0016 m/s between the 200 mesh elements and 800 mesh elements. The coarse mesh used for the air space in the thermal analysis was 200 mesh elements while the fine mesh used for the air space in the thermal analysis was 400 mesh elements. As the number of mesh elements increased, the changes in maximum temperature and maximum velocity were minimal. Because of these minimal changes, the fine/coarse meshes used and results obtained from the thermal analysis were verified. The computed values for the different mesh sizes of the vacant space can be seen in Table 9. The mesh sizes used for the vacant space can be seen in Figure 14.

Table 9. The computed values for the different mesh sizes of the vacant space.

	Max Temperature (°C)	Max Velocity (m/s)	Total Thermal Loading (W)
200 Mesh Elements	89.88	0.0508	-69.487
500 Mesh Elements	90.13	0.0524	-69.487
800 Mesh Elements	90.19	0.0524	-69.487

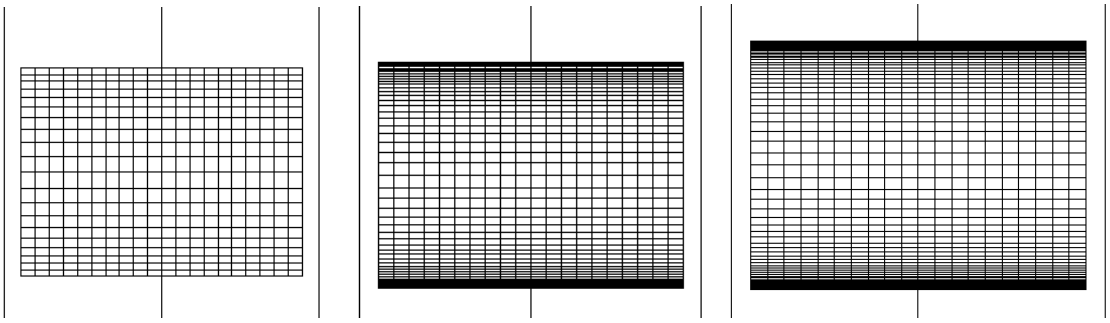

(200 Mesh Elements) (500 Mesh Elements) (800 Mesh Elements)

Figure 14. The computational meshes generated for the vacant space of the heterogeneous WP.

3.2.4 Homogeneous WP Mesh Sensitivity Analysis

A mesh sensitivity analysis was done for the Co-60 source space of the homogeneous WP case in order to verify the validity of the results that were obtained were close to being independent of mesh size. Four different mesh sizes were tested for the Co-60 source space. The mesh sizes of the Co-60 source space were 400 mesh elements, 750 mesh elements, 1640 mesh elements, and 3200 mesh elements. The maximum temperature changed 0.38 °C between 400 mesh elements and 3200 mesh elements. The coarse mesh used for the Co-60 source space in the thermal analysis was 400 mesh elements while the fine mesh used for the Co-60 source space in the thermal analysis was 1640 mesh elements. As the number of mesh elements increased, the changes in maximum temperature and maximum velocity were minimal. Because of these minimal changes, the fine/coarse meshes used and results obtained from the thermal analysis

were verified. The computed values for the different mesh sizes of the vacant space can be seen in Table 10. The mesh sizes used for the vacant space can be seen in Figures 15 and 16.

Table 10. Calculated values for the sensitivity analysis of the Co-60 source space within the homogeneous WP.

	Max Temperature (°C)	Total Thermal Loading (W)
400 Mesh Elements	88.37	69.49
750 Mesh Elements	88.63	69.49
1640 Mesh Elements	88.71	69.49
3200 Mesh Elements	88.75	69.49

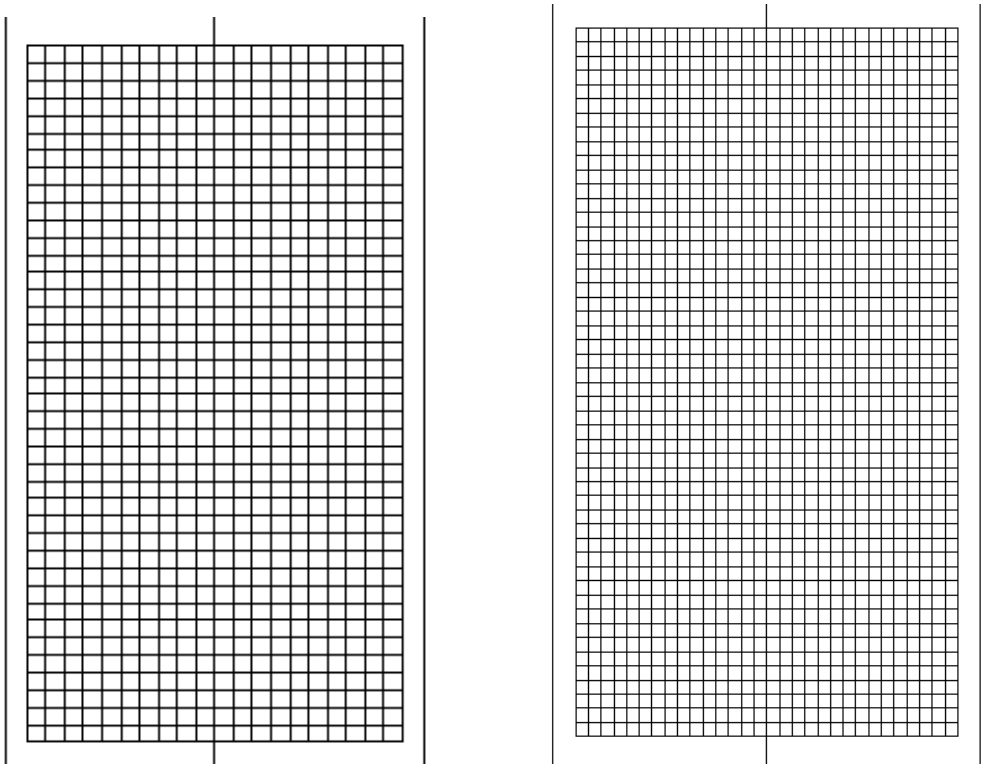

(400 Mesh Elements) (750 Mesh Elements)

Figure 15. The computational meshes generated for the Co-60 source space of the homogeneous WP.

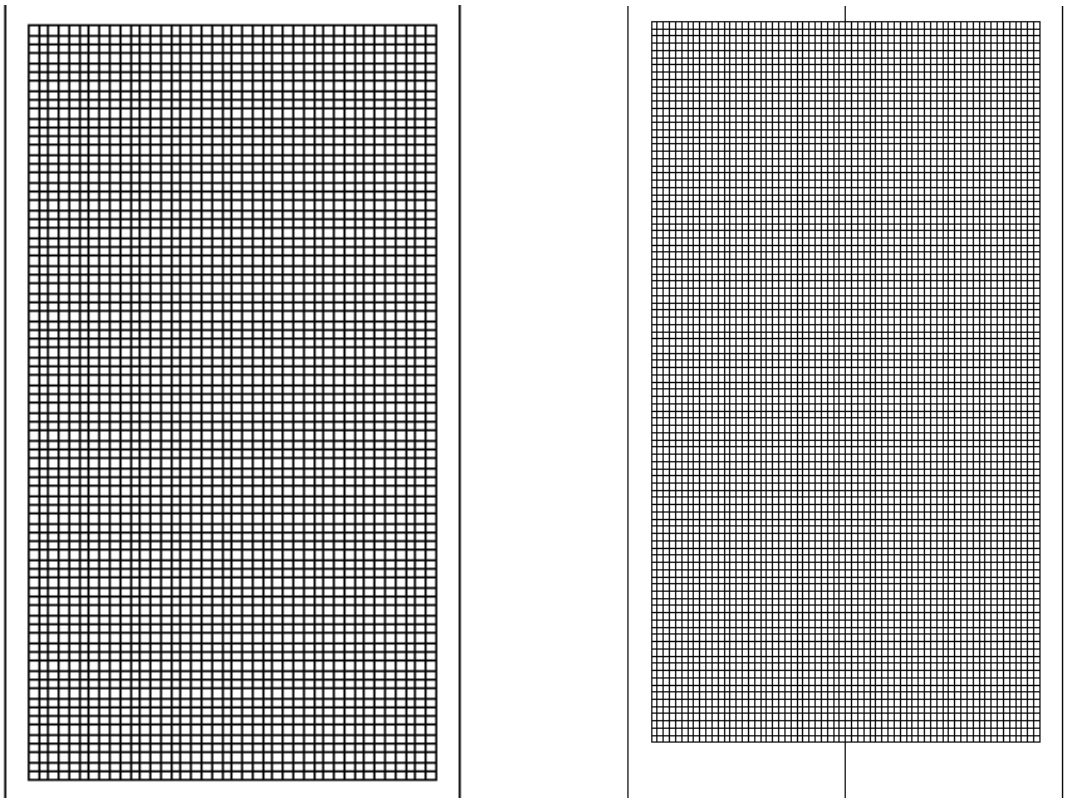

(1640 mesh elements) (3200 mesh elements)

Figure 16. The computational meshes generated for the Co-60 source space of the homogeneous WP.

4.0 Conclusions

The following conclusions were able to be drawn based on the thermal analysis of the Co-60 WP:

- The results from the CFD model and the analytical solution for the homogeneous WP in benchmarking were almost identical, which indicates that the CFD approach used here was successfully comparable to the analytical approach.
- The effect of radiation was negligible due to the low temperature gradient. The effect of natural convection was also negligible due to the small height of the air space, resulting in a low Rayleigh number (26,000). Therefore, the dominant cooling mechanism was conduction.
- Since the maximum temperature difference was minimal between the heterogeneous WP and homogeneous WP, there is indication that either WP configuration could be chosen.
- As the numbers of mesh elements increased, the changes in the maximum measured values were minimal, which indicates the fine/coarse meshes used and results obtained from the thermal analyses were verified in their mesh sizes.

5.0 References

1. IAEA, “BOSS: Borehole Disposal of Disused Sealed Sources: A Technical Manual”, 2011.
2. Preliminary study report, “Thermal Modeling for Borehole Disposal of Disused Sealed Radioactive Sources (DSRS)”, August 2016.
3. F. P. Incropera, "Appendix A: Thermophysical Properties of Matter, *Fundamentals of Heat and Mass Transfer,* Hoboken, N.J: Wiley, 2006.
4. ANSYS-FLUENT, 2009, ANSYS, Inc., Canonsburg, Pennsylvania.